Progress in Oceanography 198 (2021) 102658

Contents lists available at ScienceDirect

Progress in Oceanography

journal homepage: www.elsevier.com/locate/pocean

Bioenergetics of egg production in Northeast Atlantic mackerel changes the perception of fecundity type and annual trends in spawning stock biomass

Teunis Jansen [a,b,*], Aril Slotte [c], Thassya Christina dos Santos Schmidt [c], Claus Reedtz Sparrevohn [d], Jan Arge Jacobsen [e], Olav Sigurd Kjesbu [c]

[a] GINR (Greenland Institute of Natural Resources), Kivioq 2, PO Box 570, 3900 Nuuk, Greenland
[b] DTU AQUA (National Institute of Aquatic Resources), Kemitorvet, 2800 Kgs. Lyngby, Denmark
[c] IMR (Institute of Marine Research), PO Box 1870 Nordnes, 5817 Bergen, Norway
[d] DPPO (Danish Pelagic Producers Organisation), Axeltorv 6, 1609 Kbh. V, Denmark
[e] FAMRI (Faroe Marine Research Institute), PO Box 3051, Nóatún 1, 110 Tórshavn, Faroe Islands

ARTICLE INFO

Keywords:
Fish
Lipid
Protein
Energy acquisition
Fecundity type
Egg survey
Assessment
Reproductive cycle

ABSTRACT

Egg surveys are used worldwide for the estimation of spawning stock biomass (SSB) of small pelagic fish species, requiring detailed knowledge about their reproductive biology. In the present study, we revisit the current conceptual framework of teleost fecundity types using Northeast Atlantic (NEA) mackerel (*Scomber scombrus*) as case study due to conflicting views across different assessment methods. We hypothesized that the herein presented unique time series on protein and lipid content for this stock would help in resolving the long-lasting, intrinsic fecundity type problem. First, we document that the body surplus energy has varied substantially over time, with a significant drop to historically low levels following a stock increase from 2005 to 2015. This fluctuating pattern is in stark contrast to the stable relative fecundity (oocyte g^{-1} females) measured in connection with the egg surveys. Second, we show that the feeding levels are at the highest during the spawning season. These findings are consistent with an indeterminate fecundity type as opposed to the presently accepted determinate-type classification dating back to the 1990s. Furthermore, we quantify the batch fecundity and find it to be largely constant. Hence, the main reproductive output regulator that is driven by the bioenergetic status should therefore be the *number of batches* shed. Based on this novel framework for an indeterminate spawner, we provide alternative estimates of relative realized fecundity, which significantly change the egg survey-based SSB indices, reduces the contrast to the other data sources in the mackerel stock assessment (1990–2019), improves the assessment model fit and reduces the uncertainty of the stock size estimate. The presented algorithms and lines of thinking are applicable to other teleosts and may improve the precision and accuracy of the estimation in cases where the annual egg production method is used to assess stock size.

1. Introduction

Egg production methods (EPMs) are regularly used to assess spawning stock size (SSB) of pelagic fish species like anchovy (*Engraulis mordax*), sardine (*Sardinops sagax*), horse mackerels (*Trachurus* spp.) and Atlantic mackerel (*Scomber scombrus*) but also seeing applications on demersal species like snapper (*Pagrus auratus*), hake (*Merluccius merluccius*), cod (*Gadus morhua*) and flatfish (*Pleuronectes platessa, Solea solea*) (Bernal et al., 2012). EPMs thus play key roles in optimizing and ensuring sustainable management of several major fisheries. Furthermore, this science approach provides knowledge about key reproductive ecology aspects such as spawning phenology and distribution under varying environmental conditions, confer the highly influential CalCOFI research program in the California up-welling system (e.g. Hunter and Macewicz, 1980). In short, the EPMs consist of two main elements, namely the number of pelagic eggs (or early-stage larvae) in the spawning area and season, and the relative fecundity (number of eggs (advanced oocytes) g^{-1} females). The fact that this fecundity parameter, either further specified as relative realized fecundity (RF_R) (Annual EPM (AEPM), the present method of interest) or relative batch fecundity (RF_B) times daily spawning fraction (Daily EPM (DEPM)), appears in the denominator in the respective formulae for the resulting SSB (Armstrong

* Corresponding author at: GINR (Greenland Institute of Natural Resources), Kivioq 2, PO Box 570, 3900 Nuuk, Greenland.
E-mail address: tej@aqua.dtu.dk (T. Jansen).

https://doi.org/10.1016/j.pocean.2021.102658
Received 21 January 2021; Received in revised form 17 June 2021; Accepted 3 August 2021
Available online 9 August 2021

and Witthames, 2012) makes the precision and accuracy of reproductive information essential for the quality of the stock size assessment. Logically, a mathematically equally valid approach would be to use realized fecundity (F_R) or batch fecundity (F_B) directly in the denominator and the corresponding whole body weight (W) in the numerator (Armstrong and Witthames, 2012).

A representative presentation of F_R can be challenging because teleost fecundity and type vary with latitude, body size, migration length and ambient temperature (Kjesbu, 2016; Rijnsdorp et al., 2015), and, notably, feeding opportunities and thereby body condition (Marshall, et al. 1999; McBride et al., 2015), which may reflect the amount of atresia and thereby the level of fecundity down-regulation (Óskarsson et al., 2002). Hence, fecundity estimates should be expected to show significant individual variation across years (translating to population fecundity) due to these multifactorial influences, possibly in contrast to egg size which may appear relatively more stable (Kjesbu et al., 1991). Rationally, widely distributed species are, for practical reasons, particularly difficult to sample representatively. The question of fecundity type further complicates reproductive parameterization, the type being classified as either indeterminate ("unfixed") (typically an income breeder), determinate ("fixed") (typically a capital breeder), or an in-between combination (Ganias et al., 2015). In the determinate fish, the number of developing oocytes are settled well before the spawning season. This sum, i.e. the potential fecundity (F_P), is the maximum F_R can reach. In the indeterminate fish, this simple outline is complicated by *de novo* vitellogenesis (oocyte recruitment) during spawning. Hence, prespawning estimates of F_P are therefore, per definition, in such a situation underestimates of F_R. In order to address the difficulties in estimation of F_R by traditional snapshot counts of developing oocytes, we instead consulted proximate factors defining the level of surplus energy production (McBride et al., 2015), adopting the generally accepted principle of a positive downstream effect on oocyte production and thereby number of eggs released per gram female (Marshall, et al. 1999; Domínguez-Petit and Saborido-Rey, 2010; Kjesbu et al., 1991; Kurita et al., 2003). In particular, we focused on the role of protein and fat separately, as protein is assumingly to a larger extent supporting reproductive investment whereas fat principally covers maintenance costs (see Bradford, 1993; Kjesbu et al., 1991, and references therein). As the present application of the AEPM on the widely distributed Northeast Atlantic mackerel, hereafter referred to as NEA mackerel (or just mackerel), has turned out to be challenging to execute in a representative way due to method, time and budget constraints, questions have been raised about the robustness of the estimated SSB (see below). This research initiative therefore selected mackerel as a case study, starting out with the principal aims of potentially verifying the fecundity type and strengthening the robustness of AEPM-based SSB estimate time series by providing means to include fecundity proxies.

The mackerel SSB estimate under consideration derives from the Triennial Egg Survey, one of the largest fish surveys in the world; nine countries are covering Atlantic regions from Cádiz (Spain) in the south to Iceland in the north multiple times from February to July (ICES, 2021). However, within the last decade, these AEPM-based SSBs have been increasingly in contrast with the corresponding information from both scientific trawl and tagging surveys, as well as data from commercial catches (ICES, 2019a). This circumstance has increased uncertainty in the stock size estimate, reduced the stability and thereby reliability of the overall mackerel assessment and catch advice. Not only so, the main source for this discrepancy is unknown, even though one countermeasure has been to broaden the spatiotemporal coverage due to the currently seen northward expansion of mackerel spawning areas (ICES, 2021). Unravelling the cause and, if possible, providing a solution to this assessment problem is of uttermost priority (ICES, 2019b).

NEA mackerel body metrics, demography and population size and distribution have varied considerably through history. Mackerel are recently expanding as far as Svalbard and Southeast Greenland (Jansen, 2014; Jansen et al., 2016; Olafsdottir et al., 2019), while doubling the stock size from 2001 to 2005 to 2011–2019 (ICES, 2019a). In parallel to these changes, body condition and growth have exhibited density-dependent variability, with a strong negative trend in the latter decades (Jansen and Burns, 2015; Olafsdottir et al., 2016). For instance, in 2011–2013, 6-year old mackerel weighed approximately the same as 3-year olds in 2001–2005. Here, it is hypothesized that the decrease in body growth and condition of mackerel and thereby the poorer energy balance should have negatively affected the reproductive potential (see above). We argue that the egg survey's near-to-constant estimates of F_R and associated assumptions might be the main sources of error in the AEPM-based SSB estimate.

Before addressing fecundity proxies, there appears to be a need to revisit the current conceptual framework of fecundity type and regulation, at least regarding mackerel. The series of mackerel F_P and F_R estimates provided (ICES, 2021) are – due to the major laboratory work involved – based upon few fecundity (ovary) samples (e.g. 2016: N = 97; 2019: N = 62) in comparison to the number of sexually mature females in the whole stock (likely about 15–17 billion in the two mentioned years (ICES, 2019a)). Though, irrespective of the low numbers, the samples appear fairly well distributed in time, space and across fish sizes, and F_P (ICES, 2021) shows low variation between years (CV = 7% after the shift in methodology in 1995). A key assumption within the F_P and the following F_R estimation is that all oocytes above 185 μm are counted, a threshold that has not been rechecked over the last decades (ICES, 2021). Anyhow, this low variation in reported fecundities surprises in view of the above-mentioned large variations in body metrics and might indicate that any change in fecundity is associated with changes in number of batches (N_B) shed during the season rather than the number of eggs produced in a batch, i.e. batch fecundity (F_B). As F_R is a final, realized figure whereas F_P is a momentary figure (Ganias and Lowerre-Barbieri, 2018), the present focus was redirected towards the two factors that jointly leads to F_R, namely F_B and N_B, i.e. $F_R = F_B\, N_B$ (Ganias and Lowerre-Barbieri, 2018; Kjesbu, 2016). Essentially, interannual variation in F_B generally appears low (Charitonidou et al., 2020; Hunter and Leong, 1981; Priede and Watson, 1993), especially if accounting for variation in sampling time, because F_B likely varies markedly during the course at spawning, cf. individual Atlantic cod (*Gadus morhua*) showing a dome-shaped F_B pattern (Kjesbu et al., 1991). Hence, we hypothesize that N_B is the main dynamic reproductive investment player in mackerel rather than F_P as such as seen e.g. in cod, generally considered a determinate spawner (Kjesbu et al., 1991). This new line of thinking contrasts with the current approach where F_R is given as $F_R = F_P - AT$, with AT being loss of fecundity due to atresia (Armstrong and Witthames, 2012). Instead, we conjectured that the better the prespawning energetic condition is along with the subsequent feeding opportunities, the longer the mackerel female might continue spawning, i.e. higher N_B, reflected also by the high spawning frequency seen in this species (Charitonidou et al., 2020). In other words, developing oocytes could in theory be continuously provided from the reservoir of advanced previtellogenic oocytes (so-called PVO4c) (Serrat et al., 2019), likely quickly developing in these warm-temperate waters, going through "a near-steady F_P and F_B system" but with varying N_B. Following on from this framework, F_R might be reconstructed by dividing reproductive surplus energy with batch energy giving N_B, to be thereafter multiplied with F_B. Overall, these considerations challenge the conclusion by Greer Walker et al. (1994) that "*for all practical purposes the mackerel should be considered as having a determinate fecundity*".

In this in-depth observation-based model investigation, we start off documenting the yearly proximate composition - energetic cycle of adult mackerel based on lipid, protein, ash content, body weight and aging data from 1982 to 2019. Thereafter, we "zoom-in" on knowledge gaps that have direct implications for the egg survey-based mackerel stock assessment (and ultimately fisheries catch advice). This plan is executed by i) analysing the feeding activity during spawning that may indicate an indeterministic reproductive (income breeding) strategy), ii) evaluating the conception of approximate stability in F_B by adding new data,

and iii) linking monthly-resolved time series on adult body protein and fat (lipid) content to migration, respiration and realized fecundity. On this basis, we provide an alternative index of F_R, calculate the resulting theoretical total egg production (TEP) and SSB, and then explore how this alternative mackerel egg survey SSB index performs in the stock assessment. Hence, this investigation critically reviews and exemplifies various steps in the process of EPM-based SSBs in the interest of general principles.

2. Materials and methods

The NEA mackerel data used in this study were collected between 1982 and 2019 during pelagic and demersal trawl research surveys and from commercial fisheries, further detailed below and in Supplementary Information 1.

2.1. Lipid and protein data

An extensive international database on protein and lipid measurements of adult mackerel was compiled for the purpose of this study. The sampling program and method for measuring lipid differed among institutes and industrial data providers. Norwegian samples (1982–2019) originated from landings from the Norwegian Sea, Skagerrak and west of the British Isles (Fig. 1a, b, and c). The Norwegian Fishermen's Sales Organization for Pelagic Fish provided data from catches landed for reduction purposes (fish meal and oil). However, from the early 2000s and onwards these samples almost entirely referred to mackerel that were landed for human consumption, more specifically from the factories Pelagia Egersund (2005–2020) and Pelagia Kalvåg (2015–2019). Mackerel of typical size groups were homogenized for a given catch. In the meal and oil industry, the lipid content was measured using standard chemical procedures by heat drying, and ethyl acetate extraction of lipids (the standard Ba 3–38 method). In Pelagia Egersund and Pelagia Kalvåg, the lipid and water content were measured with near-infrared spectroscopy using Technicon Infralyzer 450. The accuracy of this instrument was maintained through regular calibration tests every catch season using the standard chemical procedures on the same samples. Results from the two sources are considered accurate and comparable (Cozzolino et al., 2002). Greenlandic Institute of Natural Resources sampled NEA mackerel in East Greenland during the International Ecosystem Summer Survey in the

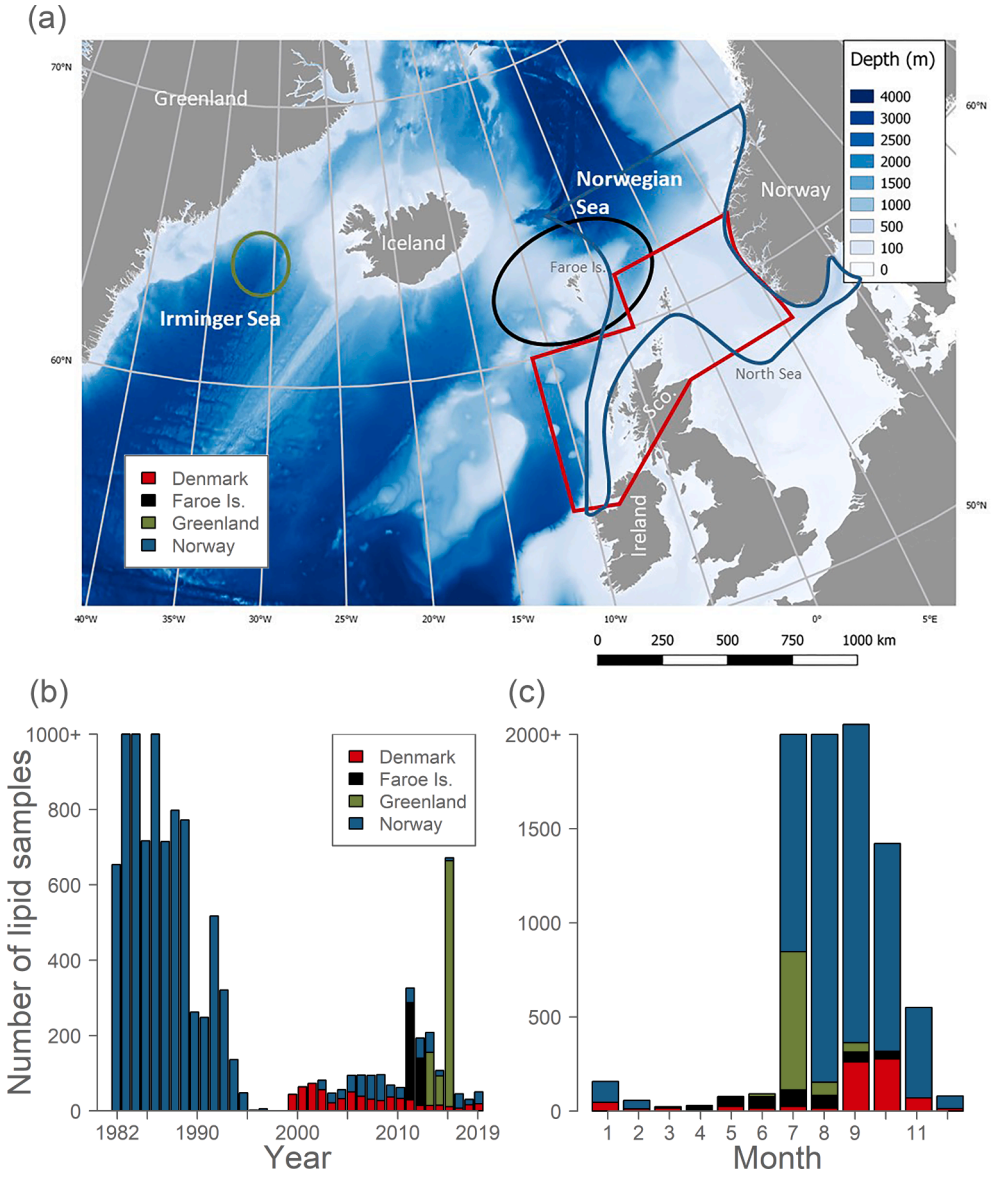

Fig. 1. Mackerel lipid samples (a) spatial distribution, (b) by year, and (c) by month. A subset of these were also analysed for protein content (see Supplementary Information 1).

Nordic Seas (IESSNS) in 2013–2015 (Fig. 1a, b, and c). Onboard, all individuals were length measured, weighed, maturity staged, and the lipid content measured above and below the lateral line on each side of the body using a Distell Fatmeter (www.fishmeatfatmetertester.co.uk) in the calibration mode "B.MACKEREL-2". The mean of the four measurements was registered as the lipid weight fraction of each individual fish. This procedure for measuring lipids was also used by the Faroe Marine Research Institute that sampled mackerel from IESSNS, scientific bottom trawl surveys and commercial fisheries around and north of the Faroe Islands zone from June to October in 2011 and from April to October in 2012 (Fig. 1a, b, and c). Finally, the Danish fish canning factory "A/S Sæby Fiske-Industri" sampled mackerel caught in 1999–2019 by commercial fishing vessels in the northern North Sea and west of Scotland (Fig. 1a, b, and c). For each catch, individual mackerel were selected three times during unloading to determine the whole body lipid content using the standard Gerber method.

The lipid content data were compiled for further statistical analyses in R (R Core Team, 2020). A test was firstly run to explore any effect of fish size on lipid content, applying a linear model on 735 mackerel, ranging from 247 to 729 g, caught off Greenland in July. This material was found particularly suitable as it referred to a well-sampled area, outside transition areas, and after the initial rapid increase in lipid content after spawning (see below). Thereafter, the lipid content (F_{Lipids}) in autumn was modelled with the purpose of estimating a time series while accounting for seasonal and area effects. Linear model fitting was done using the lm() function. The model formulation was:

$$F_{Lipids}^{bc} = \beta_0 + \beta_1 Year + \beta_2 Day + \beta_3 Area \quad (1)$$

where *Year* and *Area* were categorical factors and *Day (0 to 365)* numerical. The model was initially fitted with $bc = 1$. All parameters were statistically significant ($p < 0.05$). However, qq-plotting indicated "heavy tails" in the distribution of the residuals compared with a normal distribution. The boxcox() function from the MASS package (Venables and Ripley, 2002) was therefore used to optimize *bc* at 2.73 – all parameters were still significant and the qq-plot improved substantially.

Protein content data came solely from Norwegian Fishermen's Sales Organization for Pelagic Fish with reference to catches landed for reduction purposes (fish meal and oil) in 1982–2015 (>99% from before 1996). First, the weight of the dry matter solids relative to the wet weight was recorded as the weight after heat drying and ethyl acetate extraction of lipids. The dry matter solids consists of protein, carbohydrate and ash (skeletal material), in which the carbohydrate ($P_{Carbohydrate}$) and ash (P_{Ash}) remain relatively constant with time at approximately 5% and 1.5% of the dry weight including lipids, respectively (see Slotte, 1999 and references therein). Thus, the protein fraction of the whole body weight ($P_{Proteins}$) was calculated as:

$$P_{Proteins} = P_{Dry\_Matter\_Solids} - \left(P_{Dry\_Matter\_Solids} + MP_{Lipids}\right)\left(P_{Carbohydrate} + P_{Ash}\right) \quad (2)$$

where $P_{Dry\_Matter\_Solids}$ was the measured dry matter fraction (excluding lipids) and MP_{Lipids} was the mean lipid fraction of the whole body weight (equal weighted mean of the mean month).

2.2. Biological data from individual fish

Biological data on individual mackerel were extracted from the biological database at Institute of Marine Research (IMR). IMR routinely analyse individual mackerel from various research surveys and commercial landings, recording the following parameters: total length, whole body weight, sex, maturity stage, stomach fullness and age (from otoliths). In the present study, data were included from 140 174 mackerel (72 833 females) from 1989 to 2019. Maturity staging was according to macroscopic criteria: immature (stages 1 and 2, colourless small gonads), early maturing (stage 3, gonads opaque and less developed), late maturing (stage 4, larger gonads, oocytes can be easily seen and testes are becoming white), ripe (stage 5, large gonads, eggs are transparent and milt is a thin liquid), spawning (stage 6, running gonads), spent (stage 7, gonads are slack, may contain residual eggs or milt), and resting (stage 8, gonads are small) (Mjanger et al., 2020). Evaluation of feeding activities in terms of stomach fullness was based on the following scale: (1) empty – no content, (2) very little content – stomach needs to be cut open to check if there is any content, (3) some content – clearly visible that some content is present without cutting stomach, (4) full – stomach completely full, and (5) bursting – stomach is distended and firm (Mjanger et al., 2020).

The sex ratio (SR i.e. $N_{females}/ N_{females+males}$) was calculated for samples consisting of more than 50 individuals of 3+ years (to reduce random bias and young fish difficult to sex determine, respectively). Linear modelling was applied to test if the sex ratio was statistically different from 0.5 in any month.

To investigate seasonal variation in weight- and length-at-age, data were collated from all research surveys and commercial landings available. However, for data used to explore interannual variation in weight-at-age, and for analyses of energy loss over the reproductive cycle from autumn to spring (see below), data were further restricted to make sure they were as unbiased as possible: Slotte et al. (2007) demonstrated that survey trawl data during autumn are selective toward mackerel of small size and low condition, whereas corresponding commercial purse seine data appear representative. For this reason, the Norwegian purse seine data were used to analyse interannual variation in body condition after the feeding season ceases in autumn, spanning the starting point of the reproductive cycle (set to be 1 October, see below) (N = 9 453). The only long-term time series representing the body condition of mackerel during the spawning season in the main spawning areas along Ireland and British Isles is the IMR time series from the tagging surveys going back to the 1980 s (Tenningen et al., 2011). In this series (N = 4 997), the mackerel are collected using jigging equipment, with same sized hooks over the 40 years' time series. Although so, one cannot disregard the possibility that there may be some selectivity for total length (mouth size) but less likely so for body condition (weight at length). All age reading was conducted by the same experienced personnel at IMR, both during the autumn and spring, forming the basis for estimation of surplus energy by age. Hence there is expected to be a lower age reader bias than normally found in more international data on weight at age in the fisheries (ICES, 2018).

2.3. Bioenergetics

We adopted the general view that individuals of fish, at least in temperate waters, primarily use proteins for body growth and reproduction whereas lipid-based energy fuels swimming and maintenance costs, although lipids are also partly set aside for body growth and reproduction (see Introduction). As already well documented, somatic storing and usage of these components vary over the course of the year. The present study provides budgets for protein and lipids (in KJ) of females from autumn through winter to the spawning season in spring. This period, collectively described herein as the "reproductive cycle", begins after body growth has ceased and most gonads are macroscopically in the "resting" maturity stage, though microscopically showing signs of early maturation (vitellogenesis) (Greer Walker et al., 1994). Feeding activity (stomach fullness) by maturity stage was thereafter consulted (see Results Section), expecting seeing minimal food intake during the well-sampled months in late autumn and winter (Mehl and Westgård, 1983), while the results from months December, March and April were considered with some reservation because of the low numbers (<50) of stomachs analyzed within these months. The analysis therefore includes estimates of the reserves stored (and thereafter utilized) as either proteins ($E_{Loss\_Proteins}$) or lipids (E_{Loss_Lipids}), energy spent on respiration ($E_{Respiration}$) including activity costs, but excluding specific dynamic action, waste losses (egestion and excretion) and growth in total length (Brett and Groves, 1979). Assuming that all surplus energy is spent on reproduction,

i.e., production of developing oocytes (eggs) (E_{Eggs}), then the energy budget for proteins and lipids can be expressed as:

$$E_{Eggs\_Proteins} = E_{Loss\_Proteins} \quad (3)$$

$$E_{Eggs\_Lipids} = E_{Loss\_Lipids} - E_{Respiration} \quad (4)$$

Further assumptions, model equations and constants are provided below and in Table 1.

The energy expense egg^{-1} was calculated for the protein and lipid fractions, respectively (Table 1). The total energy content egg^{-1} (E_{Egg}), based on a general model for fish eggs with oil globules, equals $Volume_{Egg}$ (1.34 + 40.61 $P_{Egg\_Oil\ Globule}$), where $P_{Egg\_Oil\ Globule}$ is the volume fraction of the egg that is oil globule (Riis-Vestergaard, 2002). Mackerel egg diameter has been measured in the laboratory to 1.209 mm (sd = 0.029, N = 270) (Mendiola et al., 2007). This size is in line with field data from the north-west Atlantic, where the eggs were furthermore shown to decrease over the spawning season from an average of 1.3 to 1.1. mm in diameter (Gulf of Saint Lawrence; Ware, 1977). The oil globule in mackerel eggs, considered 0.31 mm in diameter (Mendiola et al., 2007), was assumed to consist of 100% lipids with a weight density of $9{\cdot}10^{-4}$ g mm^{-3} (Craik and Harvey, 1987) and an energy density (ED_{Lipid}) of 38.93 KJ g^{-1} (Jobling, 1995). Together, this corresponds to an E_{Egg} of 1.80 J; E_{Egg} equals the energy content of the oil globule plus the energy content of the egg yolk. The mackerel yolk (vitellogenin) was assumed to contain similar proportions as cod yolk (79% protein and 12.8% lipids) (Planck et al., 1971). Note here that the biochemical characterization of this large molecule appears similar across different fish (Tyler and Sumpter, 1996). From this, the dry weight of protein and lipid in the egg (DW_{egg}) became $5.24{\cdot}10^{-5}$ g by:

$$DW_{Egg} = \left(E_{Egg} - \left(W_{Egg\_Oilglobule} ED_{Lipids}\right)\right) / \left(0.79 ED_{Protein} + 0.128 ED_{Lipid}\right) \quad (5)$$

The weights of protein and lipid content egg^{-1} could then be calculated to $3.03{\cdot}10^{-5}$ g and $1.89{\cdot}10^{-5}$ g, respectively using:

$$W_{Lipid} = W_{Egg\_Oilglobule} + \left(\left(DW_{Egg} - W_{Egg\_Oilglobule}\right) 0.128\right) \quad (6)$$

$$W_{Lipid} = \left(DW_{Egg} - W_{Egg\_Oilglobule}\right) 0.79 \quad (7)$$

This corresponds to energy expenses for proteins ($E_{Egg\ Proteins}$) and lipids ($E_{Egg\ Lipids}$) at 0.72 J and 0.74 J egg^{-1}, respectively.

E_{Loss} was calculated from the whole body weights (W in grams), the fractions (P) of lipids and proteins at the start and end of the reproductive cycle and the energy density (ED in KJ gram^{-1} wet weight) as:

$$E_{Loss\_Lipids} = \left(W_{Start} P_{Start\_Lipids} - W_{End} P_{End\_Lipids}\right) ED_{Lipids} \quad (8)$$

$$E_{Loss\_Proteins} = \left(W_{Start} P_{Start\_Proteins} - W_{End} P_{End\_Proteins}\right) ED_{Proteins} \quad (9)$$

The whole body weight at the start and end of the reproductive cycle was calculated as mean weight of mackerel at maturity stage 8, i.e., "resting" from October 1 to November 15, and at maturity stage 7, i.e., "spent" from May 15 to June 15, respectively. The basis for selecting these date ranges are given in the Results Section. Weight data from October 2 to November 15 were corrected for the weight loss in October and early November (linear modelling described in Supplementary Information 2), this was done similarly for the weight data from May 16 to June 15. Spatiotemporal sampling coverage was high, only 4% of the age-year combinations were unsampled. These, primarily older and therefore numerically less important, strata were interpolated (Supplementary Information 2). The fractions of lipids at the start of the reproductive cycle was derived from linear modelling of data from September and October with Day as linear effect (visual inspection of the data did not suggest non-linearity in this period), and Year and methods as factorial effects. The chemical analyses applied to the Norwegian and Danish samples were considered accurate (see above) and the samples were largely from the same area. These data sources were therefore considered

Table 1
Model constants, equations and sources.

Element	Equations and descriptions	Value	Unit	Reference
r_{Egg}	Egg radius	0.605	mm	Mendiola et al. (2007)
D_{Water}	Density of 35 ‰ sea water at 12 °C	1.027 10^{-3}	g mm^{-3}	www.engineeringtoolbox.com/sea-water-properties-d_840.html
WW_{Egg}	Egg wet weight = (4/3) pi (r_{egg}^3) D_{Water}	9.25 10^{-4}	g	Assuming neutral buoyancy in sea water
$r_{Egg\_Oilglobule}$	Radius of the oil globule in the egg	0.31 / 2	mm	Mendiola et al. (2007)
WD_{Lipid}	Weight density of lipid	9 10^{-4}	g mm^{-3}	Craik and Harvey (1987)
$W_{Egg\_Oilglobule}$	Wet weight (=dry weight) of oil globule = ((4/3) pi ($r_{Egg\_Oilglobule}^3$) WD_{Lipid})	1.40 10^{-5}	g	Assuming spherical shape of oil globule
$P_{Egg\_Oilglobule}$	Fraction of egg wet weight that is the oil globule = $W_{Egg\_Oilglobule}$ / WW_{Egg}	1.48 10^{-2}	1	
E_{Egg}	(4/3) pi (r_{Egg}^3) (1.34 + 40.61 $F_{Egg\_Oilglobule}$)	1.80 10^{-3}	KJ	Riis-Vestergaard (2002)
ED_{Lipids}	Energy density of lipids	38.93	KJ g^{-1}	(Jobling (1995))
$ED_{Proteins}$	Energy density of proteins	23.86	KJ g^{-1}	(Jobling (1995))
DW_{Egg}	Egg dry weight = (E_{Egg} − ($W_{Egg\_Oilglobule}$ ED_{Lipids})) / (0.79 $ED_{Protein}$ + 0.128 ED_{Lipid})	5.24 10^{-5}	g	Planck et al. (1971))
W_{Lipid}	Wet weight (=dry weight) of lipids per egg = $W_{Egg\_Oilglobule}$ +((DW_{Egg} - $W_{Egg\_Oilglobule}$) 0.128)	1.89 10^{-5}	g	Planck et al. (1971)
$W_{Protein}$	Wet weight (=dry weight) of proteins per egg = (DW_{Egg} - $W_{Egg\_Oilglobule}$) 0.79	3.03 10^{-5}	g	Planck et al. (1971)
R_p	Respiration rate by phase = $\alpha W^{\beta} e^{(\rho T_p)} e^{(T_{opt} S)} ED$		KJ Day^{-1}	See MM section
p	Phase of the reproductive cycle. (See materials and methods and results)	First or second phase		This study
α	Intercept of the allometric weight function (RA) corrected for the energy equivalent of oxygen and energy density of fish, $\alpha = RA \frac{13.56}{ED}$		KJ g^{-1}	See Bachiller et al. (2018)
RA	Intercept of the allometric weight function	0.00264	g O_2 g^{-1} day^{-1}	See Bachiller et al. (2018)
ED	Energy density of mackerel = ED_{Lipids} lipid fraction + $ED_{Proteins}$ protein fraction		KJ g^{-1}	

(continued on next page)

Table 1 (*continued*)

Element	Equations and descriptions	Value	Unit	Reference
W'	Body mass = mean of weights at the start and end of the reproductive cycle.		g	This study
β	Slope of the allometric weight ($\dot{W}$) function	−0.217	g^{-1}	See Bachiller et al. (2018)
ρ	Slope for temperature (T_p) dependence; approximates the rate at which the function increases over relatively low water temperatures	0.06818	$-°C^{-1}$	See Bachiller et al. (2018)
T_p	Ambient temperature in phase p.	8.375 / 12	°C	See MM section
T_{Opt}	Optimal temperature as slope for swimming speed (S) dependence	0.0234	°C	See Bachiller et al. (2018)
S	Swimming speed calculated as counter current + distance traveled / time	28.3	cm s^{-1}	See MM section

directly comparable and grouped under the same method. The corresponding 'Faroese method' data (using Fat meter combined with sampling in a slightly different area) were estimated in the model. The few samples from Greenland in September were omitted because these fish were from the most distant summer feeding area and had not yet initiated their energy expensive migration towards the overwintering areas. This analysis could not be done for the fractions of lipids at the end of the reproductive cycle, because few years were sampled at this time of the year. The mean of all years was therefore used.

Respiration R depends on body mass, ambient temperature and swimming speed. In this study, we applied the respiration model developed for salmonids (Steward et al., 1983), further developed for application to herring (*Clupea harengus*) (Varpe et al., 2005) and mackerel (Bachiller et al., 2018). The appropriateness of using this model for mackerel was evaluated by comparing it to tank measurements of mackerel respiration (Johnstone et al., 1993). Moreover, the sensitivity of model parameter assumptions was tested by varying the parameters over plausible ranges and inspecting the impact on the results. Operationally, the respiration model provided a respiration rate by year and age for the first and second phases of the reproductive cycle (see below), respectively. These rates were then multiplied by the durations of the phases.

Adult mackerel perform extensive horizontal migrations between spawning grounds, feeding grounds and overwintering areas (Trenkel et al., 2014). During the reproductive cycle, the majority of the mackerel stock follows a distribution/migration pattern that can be generalized as consisting of two phases: 1) spawning migration and over-wintering during late autumn and winter, and 2) spawning in spring. In October and early November, the behavior and ambient temperature are highly variable. For the purpose of this study we assumed that the respiration costs were equal to those from mid-November to early March, mackerel aggregate and migrate along the continental shelf edge in the relatively warm shelf edge current, but when the water temperature gradually decreases over the season, the mackerel respond by migrating further "up-stream" and thereby maintain a relatively constant and optimal temperature (Jansen et al., 2012). All schools of mackerel observed during a study using fisheries acoustics were located within a temperature range of 7.75–9.00 °C, with the majority in 8.00–8.75 °C – no schools were observed in waters colder than 7.75 °C (Walsh et al., 1995). The ambient temperature during the first phase was therefore assumed constant at 8.375 °C (=mean of 8.00 and 8.75 °C). The previously documented interannual variation in temperature in this current could there be neglected for the purpose of this study because of the above-mentioned behavioral habit of mackerel adjusting the timing of their migration to keep the ambient temperature approximately constant. When reaching the spawning areas, the mackerel ascend to the surface waters around the time when stratification occurs due to atmospheric warming in the spring (Coombs et al., 2001; Iversen, 1977). Spawning takes place between Portugal in the south and the northern North Sea in the north, Iceland in the north-west and Sweden in the east. Spawning starts in January/February off the Iberian Peninsula and ends in July in the northern areas (Jansen and Gislason, 2013). In this study we set the shift between the two phases to the first half of March (see above). The spawning, i.e. the second phase of the reproductive cycle, happens over a vast area and during a long spawning season. However, the ambient temperature is kept within a range that is favorable for egg survival by migrating northwards as the season progress. Optimal temperatures for mackerel egg survival in experimental conditions range between 11 and 13 °C (Mendiola et al., 2006), whereas mean temperature during spawning, based on egg surveys, span 10.3 (Bruge et al., 2016), 10.5–13.5 (Ibaibarriaga et al., 2007), and 11–15 °C (Brunel et al., 2017). For the purpose of this study, the ambient temperature during spawning was set at 12 °C.

The mean swimming speed was calculated as the counter current plus the mean speed needed to migrate the distance of 1500 km from the northern North Sea to the approximate center of the spawning areas west of Ireland during the first phase of the reproductive cycle. Vertical dynamics have been shown (Fernandes et al., 2016), but the extent and bioenergetics implications are unknown and are, for the purpose of this study, assumed neglectable in relation to horizontal dynamics. The mackerel generally migrate against the current from the Northern North Sea to the spawning areas (Jansen et al., 2012). The core of the current varies substantially over short distances in space and time. It was therefore not feasible to integrate hydrographic model results over the entire time series for this purpose. Consequently, we evaluated published plots of mean current speed and direction by month from three transects across the migration route. This procedure was used to establish a "base case" current speed value. The results sensitivity to variation around this value were assessed subsequently. The first part of the route is in the Northern North Sea where the mackerel reside by swimming against the relatively warm counter current until the temperature becomes too low. During a multidisciplinary survey with focus on mackerel distribution in 1995, the speed of this current was measured to vary between 10 and 30 cm s^{-1} from September to the end of the year (Fig. 8 in Reid et al, 2001). When the mackerel leave the Northern North Sea and migrate towards southwest at the Scottish side of the Faroe-Shetland channel, they briefly encounter higher current speeds (35–60 cm s^{-1} modelled mean from 270 to 290 km along transect "SEFOS 19" in November-February 1995 (Fig. 1.3.11 in Anon, 1997)). Subsequently, along the shelf edge west of Scotland, the counter current runs at speeds of 20–35 cm s^{-1} in November-February (around 50 km along transect "SEFOS 16" (Fig. 1.3.11 in Anon, 1997)) (Anon, 1997; Reid et al., 2001). Because the mackerel typically spend substantially longer time in the Northern North Sea compared to the migration between west of Scotland and the spawning areas, we assumed a mean at 20 cm s^{-1}, used for the "base case".

2.4. Population data

The biomass of spawning females by age and year was derived from ICES' final mackerel stock assessment in 2019 (ICES, 2019a) using the following data: numbers at the beginning of the year (N), fishing mortality (FM), natural mortality (M = 0.15), fractions of FM and M happening between the start of the year and time of peak spawning

(*FMprop*, *Mprop*), mean individual weight at spawning (W_{Mean}), fraction mature (*Mat*) (Supplementary Information 3) and the sex ratio (*SR*). The biomass of spawning females by age and year at the time of spawning ($SSB_{Females}$) was calculated as:

$$SSB_{Females} = SR\ Mat\ N\ \left(1 - e^{-(Mprop*M+FMprop*FM)}\right)\ W_{Mean} \quad (14)$$

Mprop was taken from the ICES stock assessment which was based on the timing of peak spawning as measured during the Triennial Egg Survey (ICES, 2019a).

2.5. Fecundity

Realized fecundity (eggs spawned per season), based on available proteins, was calculated by age for each year as:

$$F_{R,Age} = E_{Loss\_Proteins,\ Age}/E_{Egg\_Proteins,} \quad (10)$$

and then scaled up to total stock fecundity:

$$F_{R,\ Stock} = \Sigma_{All\ Ages}\left(F_{R,\ Age}N_{Age}Mat\ SR\right) \quad (11)$$

or, following standardization by SSB, as relative total stock fecundity:

$$RF_{R,Stock} = F_{R,Stock}/SSB_{Females} \quad (12)$$

This routine was done similarly for lipids.

Relative batch fecundity, RF_B (number of developing oocyte (eggs)$^{-1}$ g^{-1} whole body weight) was presently analyzed in the IMR laboratory for 58 individuals collected during two spawning seasons: in the Norwegian Sea from May to July 2018 and West of Ireland from March to June 2019. Each individual was staged by the most advanced oocytes, following microscopic classification. Only females in final maturation, i.e., showing oocytes in migratory nucleus, germinal vesicle breakdown and hydration (Brown-Peterson et al., 2011; Lowerre-Barbieri et al., 2011) were used for batch fecundity estimation. The number of batches by spawning season were calculated as:

$$N_{B,\ age} = RF_{R,Age}/RF_B \quad (13)$$

Thus, $RF_{R,\ Age}$ is based on advanced bioenergetic considerations whereas RF_B refers to direct observational counts.

2.6. The mackerel stock assessment

Finally, the scaled-up effect of shifting from the fecundity reported by ICES to the present bioenergetically-based fecundity was considered by comparing the mackerel stock assessment by ICES in 2019 ("MackWGWIDE2019v02" in www.StockAssessment.org) to a clone of that assessment named "MackWGWIDE2019v02_Alt1". The egg survey SSB index in the clone was multiplied by F_{R_MEGS}/F_{R_New}, where F_{R_New} was the fecundity time series calculated on the basis of surplus protein available for reproduction and F_{R_MEGS} was the fecundity estimates from ICES (ICES, 2021; ICES, 2016). As this was a ratio the *W* in RF_R cancelled out.

3. Results

The entire dataset contained lipid data from 38 of the 43 years between 1982 and 2019 and from all the months of the year. However, sampling density differed substantially among years and months (Fig. 1b and c).

3.1. Lipid and protein dynamics

Totally 9 335 records of protein content from 1982 to 2015 (>99% from before 1996) were available. The annual mean protein content was 14.6% (CV = 6.8%) (Fig. 2). There was no statistical difference between the start and end of the reproductive cycle (t.test, October vs. May/June; $p = 0.37$; $df = 4$), however, there were few samples (5) from May/June.

For lipid content, 11 977 records were compiled in the database, covering the period from 1982 to 2019. In contrast to the rather stable protein content, the lipid content changed radically within the year, i.e., up to 25 percent points (Fig. 3). The lipid content decreased significantly around the beginning of the reproductive cycle (−0.021% day^{-1} during September-October, $p < 0.001$) (Fig. 3) and differed significantly across years ($p < 0.001$), though with a more or less steady decrease in the years after 2011, but ending with a moderate increase in 2019 (Fig. 4). Furthermore, the Faroese method (Fatmeter and sampling area) resulted in 0.16% lower lipid content ($p < 0.001$). The lipid content was unrelated to the body size (*W*) of adult mackerel, as measured in summer ($p = 0.7$, N = 735, data from Greenland in July, *W* range 247–729 g).

3.2. Feeding during spawning

The present stomach fullness investigation showed that mackerel feed intensively during the spawning season (mainly after March, Fig. 5a), regardless of the maturity stage (Fig. 5b,c and d). The results indicated that mackerel do not finish spawning before starting to feed; they also feed when they are in spawning activity (maturity and spawning stages (Fig. 5b)). The fraction of mackerel collected with empty stomachs has increased since 2010 (Fig. 5b and d).

3.3. Bioenergetics

Body growth differed slightly between the sexes, as both total length and whole body weight at age was slightly lower for males than for females (e.g. 0.4% in length and 2% in weight for 5 years old mackerel in October). All calculations were therefore based on data from females only. The sex ratio was not statistically different from 0.5 in any month ($p > 0.05$, N = 90606); the subsequent calculations were based on $SR = 0.5$.

The 29 744 records of macroscopic maturity stage by period and fish size (length and weight) indicated that the vast majority (98%) was "resting" (maturity stage 8) from mid-August to the end of November (Fig. 5c). Growth in weight and length ceased in late September and was followed by a declining trend in weight (Fig. 6a and b). On this basis, we assumed that all energy was used for either respiration (including swimming) or gonad development from the first of October (based on microscopic maturity staging information; see Material and Methods) to

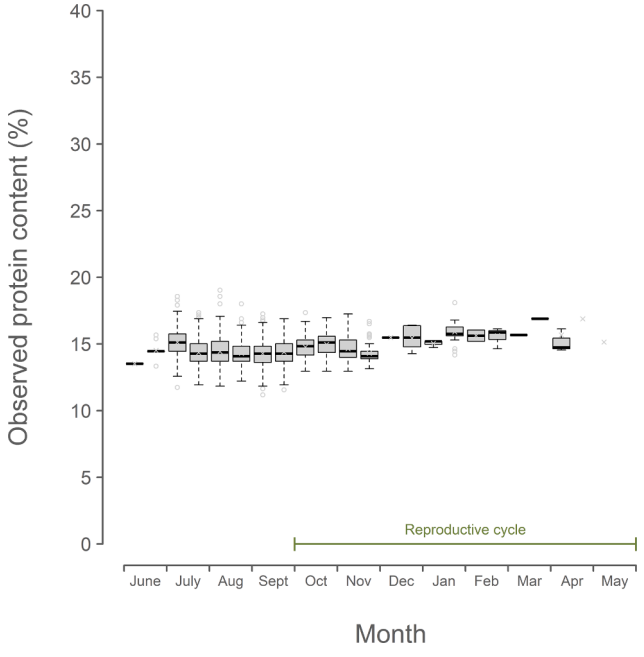

Fig. 2. Protein content year cycle by half month. Reproductive cycle (Oct-May) indicated by green line. Data from 1982 to 2015.

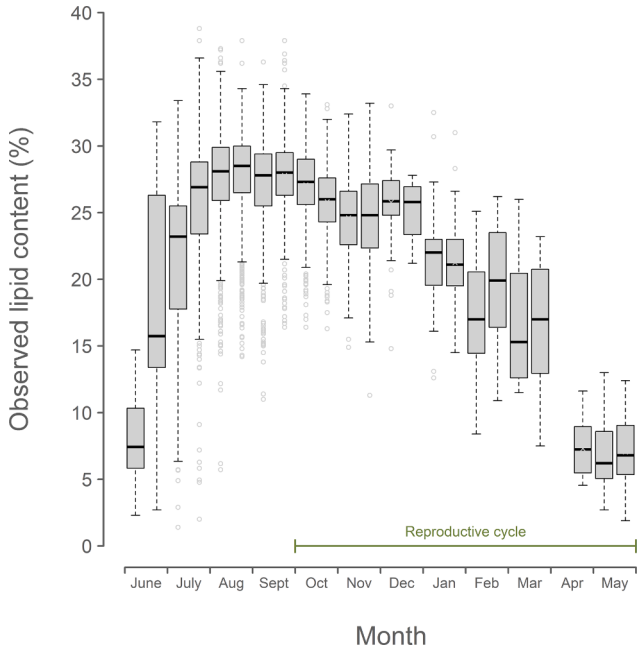

Fig. 3. Lipid content year cycle by half month. Reproductive cycle (Oct-May) indicated by green line. Data from 1982 to 2019.

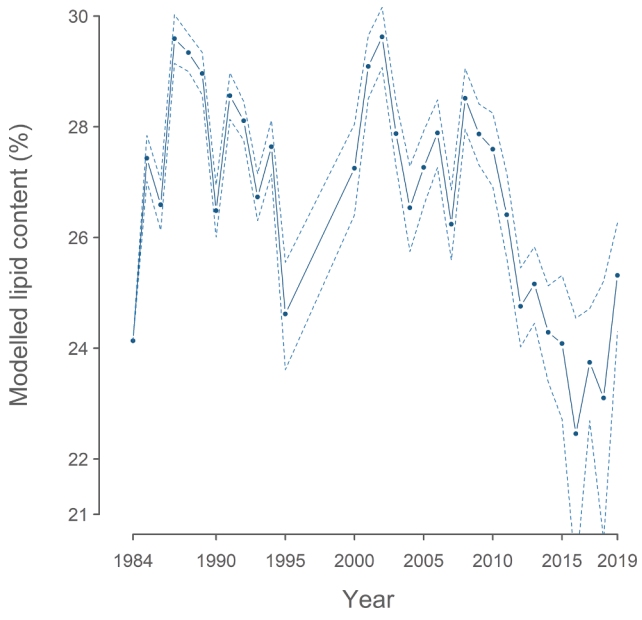

Fig. 4. Lipid content by year. Values are standardized to 1st of October using a linear model. Stippled lines indicate the 95% confidence interval.

the end of the reproductive cycle. The average end of the reproductive cycle was defined as the period when the majority of the fish were either spent or spawning, but before a substantial proportion (>25%) of the fish were macroscopically staged as resting as well as gaining body weight, i.e., the first of June (Figs. 5c, 6a and b).

The protein loss through the reproductive cycle increased by age from 15 g fish^{-1} at age 2 to a peak at 22 g at age 9 years. However, when standardized by body weight (W) at the time of spawning, the protein loss (i.e. surplus protein presumably incorporated into oocytes) decreased with age (Fig. 7a). As noticed, the protein loss in recent years was substantially lower for all ages (Fig. 7a). This shift in the later years was a consequence of the decrease in weight at age (Fig. 7b), i.e. the combined effects of growth and condition. Similarly, the surplus lipid-based energy content (before accounting for respiration) increased with age, as seen in the combined seasonal progression of weight and lipid content (Fig. 7c), but decreased with age when expressed relative to the body weight.

The respiration model was validated by comparing it to tank measurements of mackerel respiration (see Material and Methods). The energy expense estimated using the model was 11.3% lower than measured in the tanks. We found this acceptable and therefore based the further analyses of lipid-based energy on this model.

Combining the calculated surplus protein and lipid by age with the estimated stock numbers by year and age (Supplementary Information 3) provided a historic view of the egg production potential of the mackerel stock ($F_{R,\ Stock}$). The numbers of eggs that could be produced on the basis of surplus protein appeared to follow the approximate perception by ICES up to 2002 but from 2003 to 2012 being at a markedly higher level (Fig. 8a). However, between 2013 and 2019 the number of eggs that could be produced on the basis of stored proteins was undoubtedly lower than reported by ICES (Fig. 8a). The time series of lipid-based energy available for egg production indicated a modest interannual variation up to 2013 but then fell to a radically lower level in the most recent years (Fig. 8b). The lipid energy budget was negative in 18 of the 30 years indicating that additional energy was needed to sustain egg production.

When accounting for variation in spawning time, our results indicate that the mackerel had substantially less lipid-based energy left for reproduction from 2014 to 2019 (Fig. 8b). These lipid-based results were, however, strongly influenced by the assumptions about swimming (distance and current), temperature and duration of the reproductive cycle. The surplus lipid-based energy was reduced by 40% for a 6-year-old mackerel when the mean counter current was increased from 20 to 22 m s^{-1}, and 29% when the temperature in the spawning season was increased from 12 to 13 °C. So, the absolute level of the values based on lipids were considered uncertain, but given the large contrasts over time in available energy primarily due to changes in body condition and growth, we treated the time series of the lipid-based energy as a relative index assuming constant migration, current patterns and food intake over the entire time series.

3.4. Fecundity

Expressing the abovementioned results as relative realized fecundity (number of eggs (developing oocytes) g^{-1} female in the stock; $RF_{R,\ stock}$), our results suggest a different historic development than reported by ICES (Fig. 9a). This discrepancy was further elaborated on from a batch perspective: the number of realized eggs per batch relative to the body weight (RF_B) was estimated to 40.0 (95% conf. interval: 36.1 – 43.9) eggs batch^{-1} g^{-1}. No significant relation with total length was found ($p > 0.001$) (Fig. 9b). Dividing surplus-protein-based $RF_{R,\ age}$ by observational RF_B then led to the number of batches ($N_{B,\ age}$) by spawning season and age (Fig. 9c). A weighted mean $N_{B,\ Stock}$, where the weighting factor was the numbers at age, could then be calculated and presented as a time series of $N_{B,\ Stock}$ (Fig. 9c).

3.5. The mackerel stock assessment

We assumed that other physiological and behavioural constraints limit the egg production to a maximum capacity, even if food resources are optimal. This constraint must be above the RF_R measured by ICES (mean = 1134 eggs g^{-1}) (Fig. 9a). In order to explore the possible effect of our results on the stock assessment, we assumed a maximum of RF_R of 1500 eggs g^{-1} (Fig. 9a) and did not consider additional protein consumed during spawning. Replacing the fecundity time series in the ICES stock assessment of mackerel with the fecundity derived from surplus protein available for reproduction reduced the contrast between the mackerel egg survey and the other indices of adult mackerel and improved the SAM model fit to the mackerel egg survey data (Fig. 10).

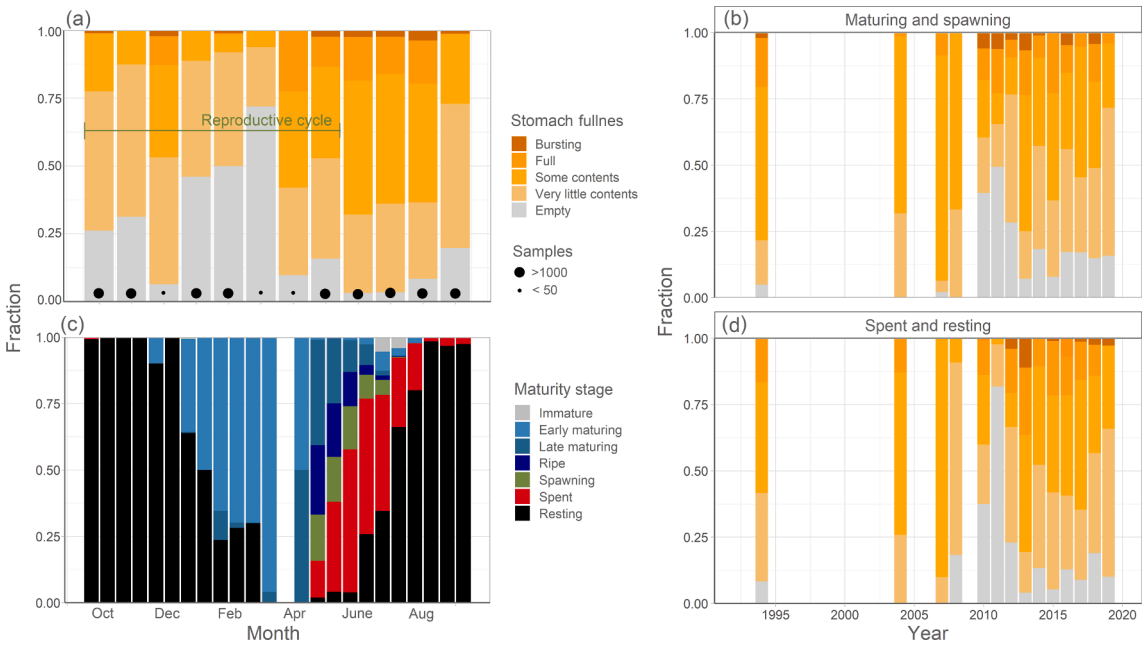

Fig. 5. Feeding and maturation information. (a) Stomach fullness of adult mackerel by month, (b) and (d) in May south of 58°N by maturity stage (see figure header) and year, and (c) maturity stage distribution by half month for 4 to 8 years old mackerel. Data collected by IMR between 1993 and 2003.

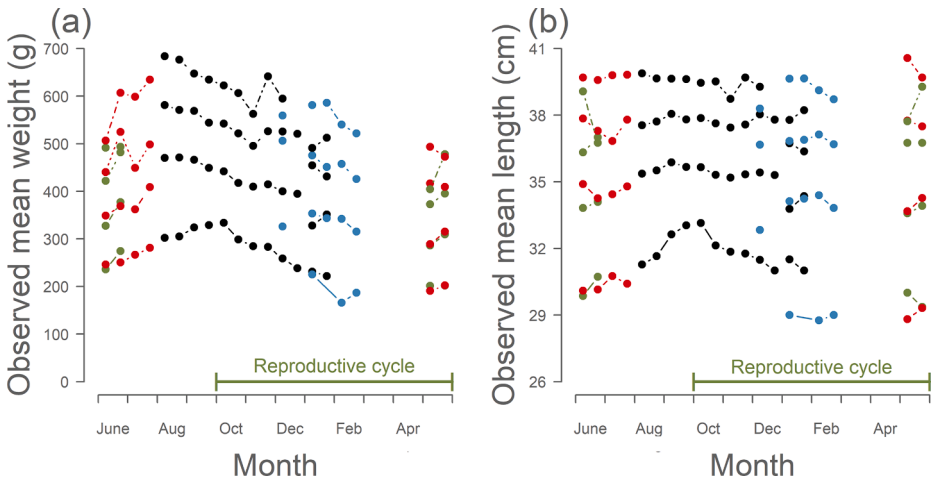

Fig. 6. (a) Whole body weight and (b) total length of 2, 4, 6 and 8 years old mackerel by half month and maturity stage (see colour scale in Fig. 5). Data collected by IMR between 1993 and 2003.

The overall SAM model fit improved (Log-Likelihood increased from −2430 to −2422 and AIC decreased from 4 913 to 4 896) and uncertainty of the stock size estimate in the most recent year decreased (i.e. the basis for the forecast used for catch advice). As a further sensitivity test, the assessment was refitted based on maximum RF_R of +/− 20%. Both runs led to better model fits (Log-Likelihood = −2422/−2424) than the original from ICES (2019). Theoretically, the assessment model could also be fitted with a time series of SSB based on RF_R from surplus lipids. However, the energy balance for lipids were more complex and thus uncertain. In most years, the energy stored as lipids was insufficient to cover the energetic expenses related to respiration and migration. The mackerel must therefore depend on food intake to balance this deficit to allow for egg release to continue.

4. Discussion and conclusion

The annual cycle of protein and lipid content was, for the first time, quantified for the ecologically and commercially highly important Northeast Atlantic mackerel using data from multiple years and areas, expanding the view that Bachiller et al. (2018) provided for the feeding season (see also brief reports on fillets in Jensen and Reimers (1979) and Wallace (1991)). Combined with data on body weight, length and stomach fullness during the reproductive cycle as well as associated batch fecundity, we addressed core aspects of this stocks reproductive biology. Our results contrast to the nearly stable expression of fecundity measured during the Triennial Egg Surveys under the currently accepted notion that mackerel is a determinate spawner. Rather, the present findings are consistent with an indeterminate fecundity type. This reclassification is to be expected as the mackerel is not only a relatively small-sized, warm-temperate species but also documented here to feed during the extensive spawning season, particularly in the end, thus an indeterminate, income breeder based on standard terminology (Rijnsdorp et al., 2015). A graphical representation of the fecundity-steering concept we propose is given in Fig. 11 for an individual in two contrasting nutritional (physiological) states; low and high levels of energy, respectively. When protein and lipid resources are available, developing

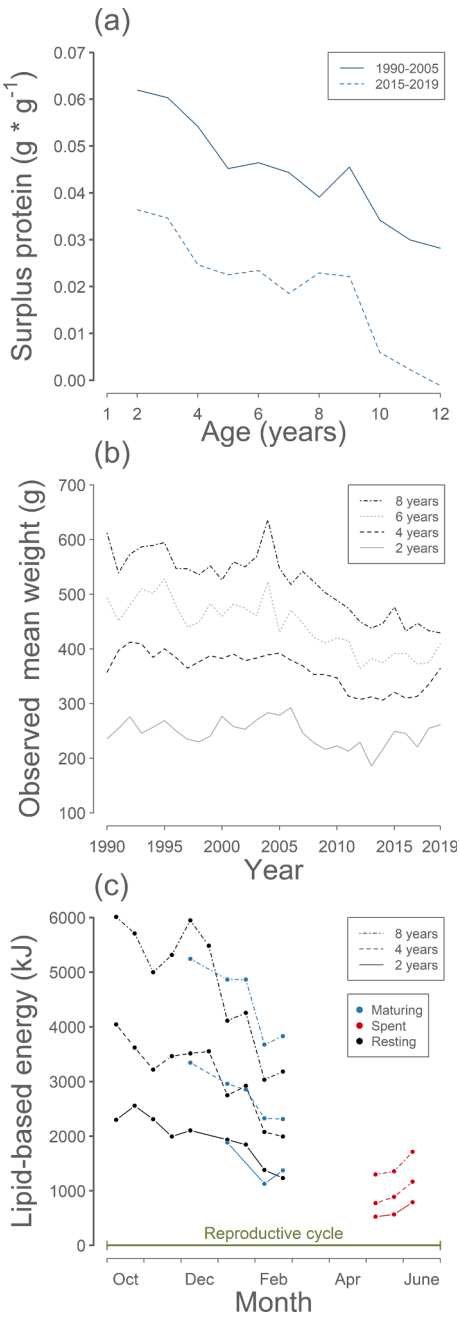

Fig. 7. Dynamics of surplus protein and lipid. (a) Surplus protein by age for two contrasting year ranges (1990–2005 vs. 2015–2019), (b) whole body weight by age and year of mackerel at the beginning of the reproductive cycle (i.e. in October the year before), and (c) mean energy content of 2, 4 and 8 years old mackerel by half month and maturity stage in 1993 – 2010.

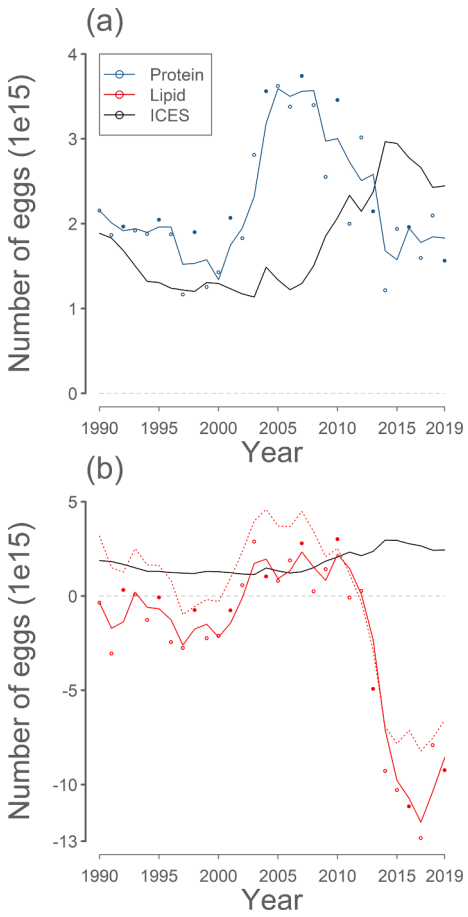

Fig. 8. Stock fecundity. Total number of eggs that could be produced by surplus energy from (a) protein and (b) lipids. Dotted red line in (b) is based on the average ending date of the reproductive cycle, while the solid red line includes the interannual variation in spawning time (Mprop). Black line indicates ICES' estimate of the female proportion of the spawning stock biomass (ICES, 2019a) times 1134 eggs per g female (the mean realized fecundity in 1998–2019). Filled circles indicate egg survey years and solid coloured lines line indicate 3-year moving averages. Note the different y-axis range in panel (a) and (b). (For interpretation of the references to colour in this figure legend, the reader is referred to the web version of this article.)

oocytes might continuously be provided from the reservoir of advanced previtellogenic oocytes (PVO4c), quickly developing and going through "an approximate steady F_P and F_B system" but varying N_B. However, especially for F_P (and F_R) this parametric stability might be called into question in the future; our current considerations incorporate that oocytes (small PVOs) above 185 μm later join the developing pool and thereby ultimately end up as eggs to be released (ICES, 2021). Also, F_B might be more varying following standardization by "stage of spawning" (Anderson et al., 2020). Furthermore, this work along with ICES data (ICES, 2021) do indicate some interannual variation in RF_B, i.e. from about 25 to 40 g^{-1}. However, the present finding that RF_B is unrelated to body size (length) speaks for that batch size variability is not a key point as such in the present framework. Anyhow, for the first time for what we consider a clear example of an indeterminate teleost, it is shown that the principal reproductive output regulator of F_R appears to be N_B, the number of batches shed, found in this study to range from around 20 up to an unknown maximum. Finally, we exemplified above the consequences of misclassification for AEPM-based SSB estimation. We assumed, for the sake of argument, that RF_R does not exceed 1500 eggs g^{-1} and have provided data that indicate an RF_B around 40 eggs g^{-1} (for 2018 and 2019) which lead to a maximum N_B of 38. Our modelled RF_R time series points to that this reproductive trait has historically been both markedly higher and lower than the adopted WG figures. This view is in better accordance with the other data sources of mackerel abundance used in the stock assessment. These results appear highly relevant for stock assessment and fisheries management advice of, not only mackerel, but also other teleosts where egg or larval surveys are used in there respects.

4.1. Hindsight

The AEPM has been applied on the mackerel stock every third year since 1977 to provide an index of SSB, supplemented in 1989 by a pilot DEPM study (Priede and Watson, 1993), motivated by reservations

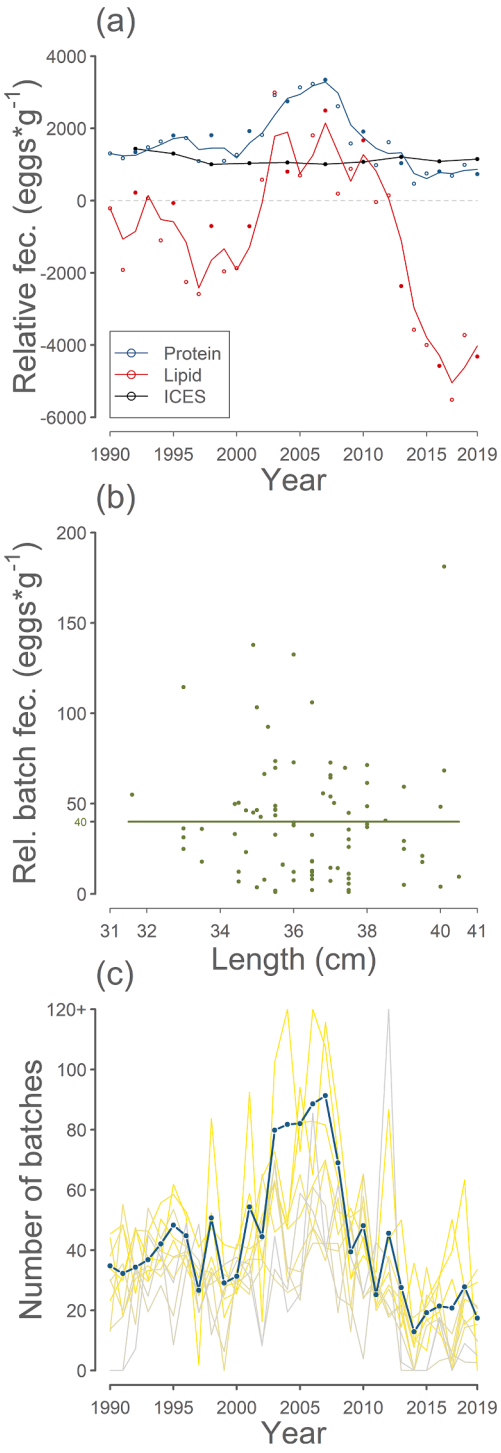

Fig. 9. Averaged reproductive traits. (a) Modelled relative realized fecundity from surplus protein and lipids, and the ICES WGMEGS estimate (ICES, 2021). Filled circles indicate egg survey years and solid coloured lines line indicate 3-year moving averages, (b) observed batch fecundity for mackerel in final oocyte maturation by total length. Solid green line indicates the mean, and (c) modelled number of batches by year (spawning season). Grey-yellow-scale lines indicate age-specific time series (yellow = older individuals) and the solid blue line shows the weighted average (weighting factor = numbers in the stock by year and age from ICES, 2019a). (For interpretation of the references to colour in this figure legend, the reader is referred to the web version of this article.)

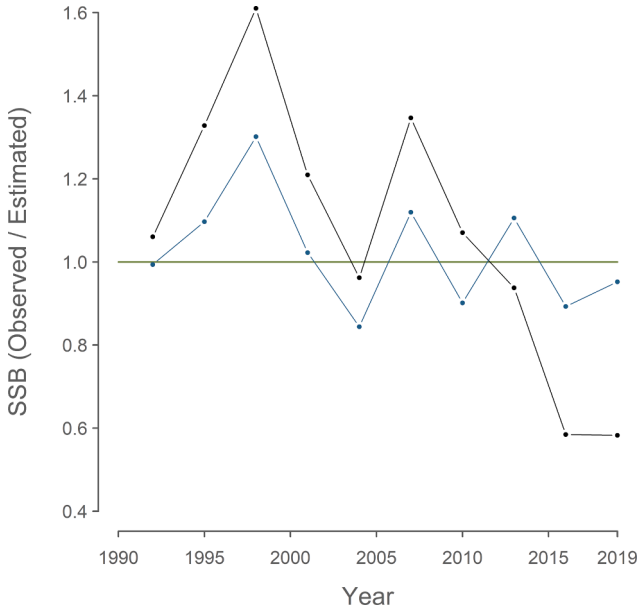

Fig. 10. AEPM SSB index relative to stock assessment model fit from ICES (2019a) (black) and the alternative from this study based on surplus protein (blue), respectively. (For interpretation of the references to colour in this figure legend, the reader is referred to the web version of this article.)

about the common opinion that the mackerel is a determinate rather than an indeterminate spawner. However, for its time, the most advanced study of Greer Walker et al. (1994) concluded that "*for all practical purposes the mackerel should be considered as having a determinate fecundity*", which paved the way for the continuation of this AEPM time series. Although Greer Walker et al. (1994) were pioneers in *de facto* incorporating PVO production as well in their fecundity type evaluations, we can today, based on the current study, say that the mackerel is highly likely an indeterminate spawner. So, "why" did earlier articles apparently misclassify the fecundity type of mackerel? Without going into too much laboratory techniques, the major "line of evidence" of Greer Walker et al. (1994) (among seven others, of which five were adopted from Hunter et al. (1989)), was that there is not enough time during the spawning season (60 days) for recruiting additional vitellogenic oocytes "to grow to full size" (140–154 days), supporting the existence of a determinate style. More specifically, the authors assumed that the oocyte growth rate in question (R_V) was similar before and during spawning, applying extrapolation, thus "fast tracking" was ruled out (Fig. 11). This consideration contrasts with the observations that multiple batch spawners display gradually increasing levels of sex steroids and vitellogenin during gonad growth but which turn into exceedingly strong pulses during spawning (e.g. Methven et al., 1992). Not only so, tracking studies of naturally spawning, "biopsied" cod females provide evidence that single oocytes may grow surprisingly quickly between successive egg batches (Kjesbu et al., 1996). Thus, R_V might be markedly higher in spawners than in prespawners.

The last decades of AEPM-based SSB estimations were, as mentioned, based on surprisingly low interannual variation in F_P (and F_R following correction for atresia). We suggest that these results were, at least partially, a consequence of measuring fecundity as a "snapshot count", i.e. without properly handling the number of actually oocytes recruiting. Thus, F_P might be expected in such a situation, based on our lines of arguments, to be approximately similar for the low and high energy situation but despite so resulting in different N_B (and thereby F_R) due to a more prolonged oocyte recruitment phase in the last case (Fig. 11).

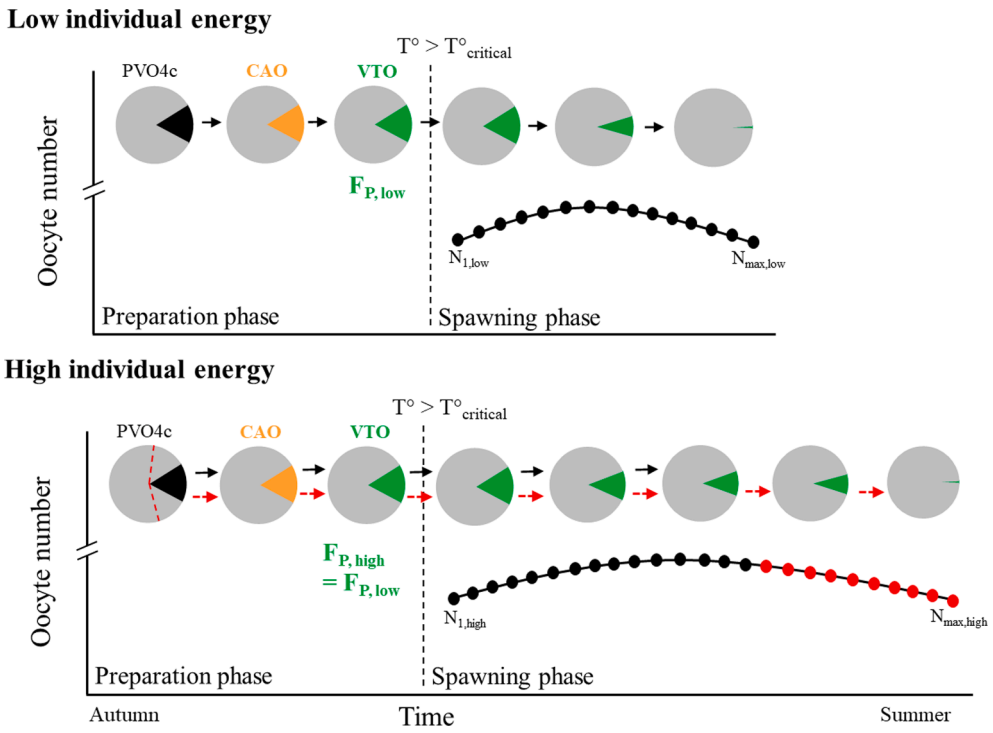

Fig. 11. Hypothesized consequences of variation in surplus energy, either low or high, on the resulting reproductive investment, i.e., here oocyte and batch number (N_B) production, of mackerel in a situation where observed potential fecundity (F_P) (cf. $F_{P,Low} = F_{P,High}$) as well as batch fecundity (see main text) seem unaffected, implying that N_B is the main response variable. Thus, in the two energy scenarios (upper and lower panel), N_B is assumed corresponding relatively low and high (using schematic figures only). In a high energy situation oocyte recruitment (red arrow) continues with a stronger strength during spawning than might be the case in a low energy situation (black arrow), a process going back to the advanced previtellogenic oocyte phase (PVO4c). As for the undertaken energetic considerations (see main text), the reproductive cycle is split (vertical line) into a preparation and spawning phase. To spawn, the ambient temperature must be above a critical temperature ($T°_{Critical}$). The presented outline is based on teleost reproductive literature review studies, foremost the "reservoir theory", where PVO4c forms the basis for the subsequently reported fecundity (Serrat et al., 2019), the "equilibrium theory", advocating that there is a state of dynamic balance between oocyte recruitment strength and egg release in indeterminate spawners, at least early on in the spawning period (Mouchlianitis et al., 2020; Schismenou et al., 2012) and, finally, the "fast track oocyte theory" (see (Rijnsdorp et al., 2015) and references therein), i.e., single oocytes may grow significantly faster than concluded from average rates seen for oocyte cohorts (Kjesbu et al., 1996). CAO = cortical alveoli oocytes; VTO = vitellogenic oocytes. The dome-shaped pattern in size from the first (B_1) to the last batch (B_1) is based on extensive research on Atlantic cod, e.g. Kjesbu et al. (1991). (For interpretation of the references to colour in this figure legend, the reader is referred to the web version of this article.)

4.2. The most recent decade

The surplus proteins and lipids available for reproduction decreased radically around 2013/2014 and remained low. Protein is, as mentioned above, assumingly to a larger extent supporting reproductive investment whereas fat principally covers maintenance costs. For this reason and because of the sensitivity to assumptions about current speeds, we based our final calculations on proteins. However, lipids are also needed for egg production and could have been the limiting factor in recent years, further supporting our conclusions. In fact, the number of eggs that could be produced from surplus energy from lipids were negative (Fig. 8b), meaning that the energetic costs for respiration were higher than the energy available in the body as lipids. This energy deficit underlines the need for feeding during the reproductive cycle and raises the question if more intensive feeding in the later years could have balanced the energetic status, and thereby led to the observed near-constant F_P estimated as a part of the old AEPM? However, this explanation seems unlikely because the depiction is rather a period with increased competition for food in a larger stock with density-dependent growth inhibition: the tendency in stomach fullness in the recent decade is negative rather than positive (Fig. 5b). As a potential negative feedback loop, the predation on the spawned eggs could potentially have increased (Olaso et al., 2005). Furthermore, the poorer energetic state of the mackerel stock was observed while the stock was large; food availability decreased likely as a consequence of top down effects (Bachiller et al., 2018; Jansen and Burns, 2015; Olafsdottir et al., 2016) and bottom up effects, e.g. from a decrease in silicate (Pacariz et al., 2016). Also, the mackerel's geographical expansion (Nøttestad et al., 2016; Olafsdottir et al., 2019) has increased the energetic cost of the summer migration. Bioenergetic status has been found to affect total egg production and recruitment for some fish stocks (e.g. Marshall et al. 1999; Takasuka et al. 2021). Surprisingly, the decrease in mackerel fecundity does not yet appear to have affected recruitment negatively (ICES, 2021; Jansen et al., 2015), likely because other factors, such as feeding opportunities for the early life stages may be main drivers (Jansen, 2016; Brosset et al, 2020).

4.3. Future perspectives

Regarding the consequences for the existing mackerel AEPM time series, undoubtedly, the value of such a long time series is unquestionable in itself. Besides, switching entirely to the DEPM seems not straightforward in the case of mackerel as it has still unresolved problems when it comes to quantifying e.g. spawning frequency, a key parameter, in an unbiased way (Charitonidou et al., 2020), as well as likely seeing spatial heterogeneity at spawning grounds (Gonçalves et al., 2009). Hence, a main route forward seems to be to focus on how to improve F_R as part of the AEPM time series, among other aspects, in parallel with the current effort to test and possibly fully implement the DEPM (ICES, 2021). Thus, likely future research activities may be guided by the present "energy-based approach", even though it requires additional dedicated analyses to be properly incorporated in the WG assessment.

Further to these elaborations, changes in relative fecundity and total egg production as such can also be expected to have implications for productivity and thereby sustainable management of exploited fish stocks. For many fish stocks, limit reference points are set to reflect when recruitment will be impaired if spawning stock biomass falls below. The logic being that the spawning stock biomass reflects the spawning capacity adequately. However, this link might be much more complex if large changes in relative fecundity take place and are not properly accounted for.

Declaration of Competing Interest

The authors declare that they have no known competing financial interests or personal relationships that could have appeared to influence the work reported in this paper.

Acknowledgements

We wish to thank the lab and field technicians from the involved institutes that sampled and measured the many mackerel analyzed in the present study. We also thank the industry partners: A/S Sæby Fiske-Industri, Pelagia Egersund and Pelagia Kalvåg, who provided historical lipid data. This study was carried out as part of the project "Sustainable multi-species harvest from the Norwegian Sea and adjacent ecosystems" funded by the Research Council of Norway (project number 299554). Furthermore, financial support was received for fat measurements in 2011 and 2012 from the Faroese Research Fund (project "Fiti í makreli", FVG nr. 11/01437) and from the Faroese Pelagic Organization "Felagið Nótaskip". This work was also supported by the European Maritime and Fisheries Fund and The Danish Fisheries Agency (33112-P-19-066), the H2020 PANDORA project (773713) as well as the Norwegian Fisheries Research Sales Tax System (FFA) (IMR project no. 15205: Climate and Vital Rates of Marine Stocks).

Appendix A. Supplementary material

Supplementary data to this article can be found online at https://doi.org/10.1016/j.pocean.2021.102658.

References

Anderson, K.C., Alix, M., Charitonidou, K., Thorsen, A., Thorsheim, G., Ganias, K., Schmidt, T.C.D., Kjesbu, O.S., 2020. Development of a new 'ultrametric' method for assessing spawning progression in female teleost serial spawners. Scientific Reports 10, 13, doi:10.1038/s41598-020-66601-w.

Anon, 1997. SEFOS, Shelf Edge Fisheries and Oceanography Study. Final Rep. May 1997.

Armstrong, M.J., Witthames, P.R., 2012. Developments in understanding of fecundity of fish stocks in relation to egg production methods for estimating spawning stock biomass. Fish Res 117-118, 35–47.

Bachiller, E., Utne, K.R., Jansen, T., Huse, G., MacKenzie, B.R., 2018. Bioenergetics modeling of the annual consumption of zooplankton by pelagic fish feeding in the Northeast Atlantic. PLoS ONE 13 (1), e0190345. https://doi.org/10.1371/journal.pone.0190345.

Bernal, M., Somarakis, S., Witthames, P.R., van Damme, C.J.G., Uriarte, A., Lo, N.C.H., Dickey-Collas, M., 2012. Egg production methods in marine fisheries: an introduction. Fish Res 117-118, 1–5.

Bradford, R.G., 1993. Differential utilization of storaage lipids and storage proteins by Northwest Atlantic herring (*Clupea harengus harengus*). J. Fish Biol. 43, 811–824.

Brett, J.R., Groves, T.D.D., 1979. Physiological energetics. Hoar, W. S., al., Eds.), Fish Physiol. Vol. 8. Acad. Press. New York/San Fr. 279–344.

Brosset, P., Smith, A.D., Plourde, S., Castonguay, M., Lehoux, C., Van Beveren, E., 2020. A fine-scale multi-step approach to understand fish recruitment variability. Sci. Rep. 10, 14. https://doi.org/10.1038/s41598-020-73025-z.

Brown-Peterson, N.J., Wyanski, D.M., Saborido-Rey, F., Macewicz, B.J., Lowerre-Barbieri, S.K., 2011. A standardized terminology for describing reproductive development in fishes. Mar. Coast. Fish. Dyn. Manag. Ecosyst. Sci. 3 (1), 52–70.

Bruge, A., Alvarez, P., Fontán, A., Cotano, U., Chust, G., 2016. Thermal niche tracking and future distribution of atlantic mackerel spawning in response to ocean warming. Front. Mar. Sci. 3, article 86. https://doi.org/10.3389/fmars.2016.00086.

Brunel, T., van Damme, C.J.G., Samson, M., Dickey-Collas, M., 2018. Quantifying the influence of geography and environment on the northeast Atlantic mackerel spawning distribution. Fish. Oceanogr. 27 (2), 159–173. https://doi.org/10.1111/fog.2018.27.issue-210.1111/fog.12242.

Charitonidou, K., Kjesbu, O.S., Dominguez-Petit, R., Garabana, D., Korta, M.A., Santos, M., van Damme, C.J.G., Thorsen, A., Ganias, K., 2020. Contrasting post-ovulatory follicle production in fi shes with diff erent spawning dynamics Fish. Res. 231, 105710. https://doi.org/10.1016/j.fishres.2020.105710.

Coombs, S.H., Morgans, D., Halliday, N.C., 2001. Seasonal and ontogenetic changes in the vertical distribution of eggs and larvae of mackerel (*Scomber scombrus* L.) and horse mackerel (*Trachurus trachurus* L.). Fish Res 50 (1-2), 27–40.

Cozzolino, D., Murray, I., Scaife, J.R., 2002. Near infrared reflectance spectroscopy in the prediction of chemical characteristics of minced raw fish. Aquac. Nutr. 8, 1–6.

Craik, J.C.A., Harvey, S.M., 1987. The causes of buoyancy in eggs of marine teleosts. J. Mar. Biol. Assoc. UK 67 (1), 169–182.

Domínguez-Petit, R., Saborido-Rey, F., 2010. New bioenergetic perspective of European hake (*Merluccius merluccius* L.) reproductive ecology. Fish. Res. 104 (1-3), 83–88.

Fernandes, P.G., Copland, P., Garcia, R., Nicosevici, T., Scoulding, B., 2016. Additional evidence for fisheries acoustics: small cameras and angling gear provide tilt angle distributions and other relevant data for mackerel surveys. ICES. J. Mar. Sci. J. du Cons. 73, 2009–2019. https://doi.org/10.1093/icesjms/fsw091.

Ganias, K., Lowerre-Barbieri, S., 2018. Oocyte recruitment and fecundity type in fishes: Refining terms to reflect underlying processes and drivers. Fish Fish. 19 (3), 562–572.

Ganias, K., Lowerre-Barbieri, S.K., Cooper, W., 2015. Understanding the determinate-indeterminate fecundity dichotomy in fish populations using a temperature dependent oocyte growth model. J. Sea Res. 96, 1–10.

Gonçalves, P., Costa, A.M., Murta, A.G., 2009. Estimates of batch fecundity and spawning fraction for the southern stock of horse mackerel (Trachurus trachurus) in ICES Division IXa. ICES J Mar Sci 66, 617–622.

Greer Walker, M., Witthames, P.R., Bautista de los Santos, I., 1994. Is the fecundity of the Atlantic mackerel (*Scomber sombrus*: Scombridae) determinate? Sarsia 79, 13–26.

Hunter, J.R., Leong, R., 1981. The spawning energetics of female northern anchovy, Engraulis mordax. Fish. Bull. 79, 215–230.

Hunter, J.R., Macewicz, B.J., 1980. Sexual maturity, batch fecundity, spawning frequency, and temporal pattern of spawning for the northern anchovy, *Engraulis mordax*, during the 1979 spawning season. Calif. Coop. Ocean. Fish. Invest. Rep. 21, 139–149.

Hunter, J.R., Macewicz, B.J., Kimbrell, C.A., 1989. Fecundity and other aspects of the reproduction of sablefish, *Anoplopoma fimbria*, in central California waters. Calif. Coop. Ocean. Fish. Investig. Reports 30, 61–72.

Ibaibarriaga, L., Irigoien, X., Santos, M., Motos, L., Fives, J.M., Franco, C., De Lanzos, A. L., Acevedo, S., Bernal, M., Bez, N., Eltink, G., Farinha, A., Hammer, C., Iversen, S.A., Milligan, S.P., Reid, D.G., 2007. Egg and larval distributions of seven fish species in north-east Atlantic waters. Fish Ocean. 16, 284–293.

ICES, 2019a. Working Group on Widely Distributed Stocks (WGWIDE). ICES Sci. Reports 1, 948. https://doi.org/10.17895/ices.pub.5574.

ICES, 2019b. Workshop on a Research Roadmap for Mackerel (WKRRMAC). ICES Sci, Reports, p. 1.

ICES, 2018. Report of the Workshop on Age Estimation of Atlantic Mackerel (Scomber scombrus)(WKARMAC2). ICES C. 2018/EOSG32 96 pp.

ICES, 2016. Surveys Second Interim Report of the Working Group on Mackerel and Horse Mackerel Egg Surveys (WGMEGS), By correspondance. SSGIEOM:09 16.

Iversen, S.A., 1977. Spawning, egg production and stock size of mackerel (Scomber scombrus L.) in the North Sea 1968-1975. ICES C. 1977/ H17.

Jansen, Teunis, 2016. First-year survival of North East Atlantic mackerel (Scomber scombrus) from 1998 to 2012 appears to be driven by availability of *Calanus*, a preferred copepod prey. Fish. Oceanogr. 25 (4), 457–469. https://doi.org/10.1111/fog.2016.25.issue-410.1111/fog.12165.

ICES, 2021. Working group on mackerel and horse mackerel egg survey (WGMEGS: outputs from 2020 meeting). ICES Sci. Reports 3 (11), 88 pp.

Jansen, T., 2014. Pseudocollapse and rebuilding of North Sea mackerel (*Scomber scombrus*). ICES J. Mar. Sci. 71, 299–307. https://doi.org/10.1093/icesjms/fst148.

Jansen, T., Burns, F., 2015. Density dependent growth changes through juvenile and early adult life of North East Atlantic mackerel (*Scomber scombrus*). Fish Res 169, 37–44. https://doi.org/10.1016/j.fishres.2015.04.011.

Jansen, Teunis, Campbell, Andrew, Kelly, Ciarán, Hátún, Hjálmar, Payne, Mark R., Peck, Myron, 2012. Migration and Fisheries of North East Atlantic Mackerel (*Scomber scombrus*) in Autumn and Winter. PLoS ONE 7 (12), e51541. https://doi.org/10.1371/journal.pone.0051541.

Jansen, Teunis, Gislason, Henrik, Goldstien, Sharyn Jane, 2013. Population structure of atlantic mackerel (*Scomber scombrus*). PLoS ONE 8 (5), e64744. https://doi.org/10.1371/journal.pone.0064744.

Jansen, T., Kristensen, K., van der Kooij, J., Post, S., Campbell, A., Utne, K.R., Carrera, P., Jacobsen, J.A., Gudmundsdottir, A., Roel, B.A., Hatfield, E.M.C., 2015. Nursery areas and recruitment variation of North East Atlantic mackerel (*Scomber scombrus*). ICES J. Mar. Sci. 72 (6), 1779–1789. https://doi.org/10.1093/icesjms/fsu186.

Jansen, Teunis, Post, Søren, Kristiansen, Trond, Óskarsson, Guðmundur J., Boje, Jesper, MacKenzie, Brian R., Broberg, Mala, Siegstad, Helle, 2016. Ocean warming expands habitat of a rich natural resource and benefits a national economy. Ecol. Appl. 26 (7), 2021–2032. https://doi.org/10.1002/eap.1384.

Jensen, J.G., Reimers, K.H., 1979. Årstidsvariationer hos makrel olie protein og tørstof. Rep. from Fisk. forsøgslaboratorium 11.

Jobling, M., 1995. Fish bioenergetics. Oceanogr. Lit. Rev. 9, 785.

Johnstone, A.D.F., Wardle, C.S., Almatar, S.M., 1993. Routine respiration rates of Atlantic mackerel, *Scomber scombrus* L., and herring, *Clupea harengus* L., at low activity levels. J Fish Biol 42 (1), 149–151.

Kjesbu, O.S., 2016. Applied fish reproductive biology: contribution of individual reproductive potential to recruitment and fisheries management. Jakobsen, T., al., Eds.), Fish Reprod. Biol. Implic. Assess. Manag. Vol. 2nd. Ed. John Wiley Sons Ltd., Chichester, UK 321–366.

Kjesbu, O.S., Klungsøyr, J., Kryvi, H., Witthames, P.R., Greer Walker, M., 1991. Fecundity, atresia, and egg size of captive Atlantic cod (Gadus morhua) in relation to proximate body composition. Can. J. Fish. Aquat. Sci. 48, 2333–2343.

Kjesbu, O.S., Kryvi, H., Norberg, B., 1996. Oocyte size and structure in relation to blood plasma steroid hormones in individually monitored, spawning Atlantic cod. J. Fish Biol. 49, 1197–1215.

Kurita, Y., Meier, S., Kjesbu, O.S., 2003. Oocyte growth and fecundity regulation by atresia of Atlantic herring (*Clupea harengus*) in relation to body condition throughout the maturation cycle. J. Sea Res. 49, 203–219. https://doi.org/10.1016/S1385-1101(03)00004-2.

Lowerre-Barbieri, Susan K., Brown-Peterson, Nancy J., Murua, Hilario, Tomkiewicz, Jonna, Wyanski, David M., Saborido-Rey, Fran, 2011. Emerging issues and methodological advances in fisheries reproductive biology. Mar. Coast. Fish. Dyn. Manag. Ecosyst. Sci. 3 (1), 32–51.

Marshall, C. Tara, Yaragina, Nathalia A., Lambert, Yvan, Kjesbu, Olav S., 1999. Total lipid energy as a proxy for total egg production by fish stocks. Nature 402 (6759), 288–290. https://doi.org/10.1038/46272.

McBride, Richard S, Somarakis, Stylianos, Fitzhugh, Gary R, Albert, Anu, Yaragina, Nathalia A, Wuenschel, Mark J, Alonso-Fernández, Alexandre, Basilone, Gualtiero, 2015. Energy acquisition and allocation to egg production in relation to fish reproductive strategies. Fish Fish. 16 (1), 23–57.

Mehl, S., Westgård, T., 1983. The diet and consumption of mackerel in the North Sea (a preliminary report). ICES C. 1983/H34.

Mendiola, D., Alvarez, P., Cotano, U., Etxebeste, E., de Murguia, A. Martínez, 2006. Effects of temperature on development and mortality of Atlantic mackerel fish eggs. Fish Res 80 (2-3), 158–168.

Mendiola, D., Alvarez, P., Cotano, U., Martínez de Murguía, A., 2007. Early development and growth of the laboratory reared north-east Atlantic mackerel *Scomber scombrus* L. J. Fish Biol. 70 (3), 911–933. https://doi.org/10.1111/j.1095-8649.2007.01355.x.

Methven, David A., Crim, Laurence W., Norberg, Birgitta, Brown, Joseph A., Goff, Gregory P., Huse, Ingvar, 1992. Seasonal reproduction and plasma levels of sex steroids and vitellogenin in Atlantic halibut (*Hippoglossus hippoglossus*). Can. J. Fish. Aquat. Sci. 49 (4), 754–759.

Mjanger, H., Svendsen, B.V., Senneset, H., Fuglebakk, E., Skage, M.L., Diaz, J., Johansen, G.O., Vollen, T., 2020. Handbook for sampling fish, crustaceans and other invertebrates. Inst. Mar. Res. 1–157.

Mouchlianitis, Foivos Alexandros, Minos, George, Ganias, Kostas, 2020. Timing of oocyte recruitment within the ovulatory cycle of Macedonian shad, *Alosa macedonica*, a batch spawning fish with indeterminate fecundity. Theriogenology 146, 31–38.

Nøttestad, Leif, Utne, Kjell R., Óskarsson, Guðmundur J., Jónsson, Sigurdur Þ., Jacobsen, Jan Arge, Tangen, Øyvind, Anthonypillai, Valantine, Aanes, Sondre, Vølstad, Jon Helge, Bernasconi, Matteo, Debes, Høgni, Smith, Leon, Sveinbjörnsson, Sveinn, Holst, Jens C., Jansen, Teunis, Slotte, Aril, 2016. Quantifying changes in abundance, biomass, and spatial distribution of Northeast Atlantic mackerel (*Scomber scombrus*) in the Nordic seas from 2007 to 2014. ICES J. Mar. Sci. 73 (2), 359–373. https://doi.org/10.1093/icesjms/fsv218.

Olafsdottir, A., Slotte, A., Jacobsen, J.A., Óskarsson, G., Utne, K., Nøttestad, L., 2016. Changes in weight-at-length and size-at-age of mature Northeast Atlantic mackerel (Scomber scombrus) from 1984 to 2013: effects of mackerel stock size and herring (Clupea harengus) stock size. ICES J. Mar. Sci. 73, 1255–1265.

Olafsdottir, A.H., Utne, K.R., Jacobsen, J.A., Jansen, T., Óskarsson, G.J., Nøttestad, L., Elvarsson, B.Þ., Broms, C., Slotte, A., 2019. Geographical expansion of Northeast Atlantic mackerel (Scomber scombrus) in the Nordic Seas from 2007 to 2016 was primarily driven by stock size and constrained by low temperatures. Deep. Res. Part II Top. Stud. Oceanogr. 159. DOI: 10.1016/j.dsr2.2018.05.023.

Olaso, Ignacio, Gutiérrez, José L., Villamor, Begoña, Carrera, Pablo, Valdés, Luis, Abaunza, Pablo, 2005. Seasonal changes in the north-eastern Atlantic mackerel diet (*Scomber scombrus*) in the north of Spain (ICES Division VIIIc). J. Mar. Biol. Assoc. United Kingdom 85 (2), 415–418.

Óskarsson, G.J., Kjesbu, O.S., Slotte, A., 2002. Predictions of realised fecundity and spawning time in Norwegian spring-spawning herring (*Clupea harengus*). J. Sea Res. 48 (1), 59–79.

Pacariz, S. V., Hátún, H., Jacobsen, J.A., Johnson, C., Eliasen, S., Rey, F., 2016. Nutrient-driven poleward expansion of the Northeast Atlantic mackerel (Scomber scombrus) stock: A new hypothesis. Elem. Sci. Anthr. 4. DOI: 10.12952/journal.elementa.000105.

Planck, P.A., Pritchard, D.J., Fraser, N.W., 1971. Egg proteins in cod serum. Biochem. J. 121, 847–856.

Priede, I.G., Watson, J.J., 1993. An evaluation of the daily egg production method for estimating biomass of Atlantic mackerel (Scomber scombrus). Bull. Mar. Sci. Vol. 53, Univ. Aberdeen, Dep. Zool., Tillydrone Ave., Aberdeen, AB9 2TN, UK.

R Core Team, 2020. R: A Language and Environment for Statistical Computing. R Found. Stat. Comput. Vienna, Austria. URL https//www.R-project.org/.

Reid, D.G., Walsh, M., Turrell, W.R., 2001. Hydrography and mackerel distribution on the shelf edge west of the Norwegian deeps. Fish Res. 50 (1-2), 141–150.

Riis-Vestergaard, J., 2002. Energy density of marine pelagic fish eggs. J. Fish Biol. 60 (6), 1511–1528. https://doi.org/10.1111/jfb.2002.60.issue-610.1111/j.1095-8649.2002.tb02444.x.

Rijnsdorp, A.D., van Damme, C.J.G., Witthames, P.R., 2015. Ecology of reproduction. Gibson, R. N., al., Eds.), Flatfishes Biol. Exploit. John Wiley Sons, Ltd. 101–131.

Schismenou, Eudoxia, Somarakis, Stylianos, Thorsen, Anders, Kjesbu, Olav S., 2012. Dynamics of de novo vitellogenesis in fish with indeterminate fecundity: an application of oocyte packing density theory to European anchovy, *Engraulis encrasicolus*. Mar. Biol. 159 (4), 757–768.

Serrat, A., Saborido-Rey, F., Garcia-Fernandez, C., Munoz, M., Lloret, J., Thorsen, A., Kjesbu, O.S., 2019. New insights in oocyte dynamics shed light on the complexities associated with fish reproductive strategies. Sci. Rep. 9, 18411.

Slotte, A., 1999. Differential utilization of energy during wintering and spawning migration in Norwegian spring-spawning herring. J. Fish Biol. 54 (2), 338–355. https://doi.org/10.1111/jfb.1999.54.issue-210.1111/j.1095-8649.1999.tb00834.x.

Slotte, A., Skagen, D., Iversen, S.A., 2007. Size of mackerel in research vessel trawls and commercial purse-seine catches: implications for acoustic estimation of biomass. ICES J Mar Sci 64, 989–994.

Stewart, Donald J., Weininger, David, Rottiers, Donald V., Edsall, Thomas A., 1983. An energetics model for lake trout, *Salvelinus namaycush*: application to the Lake Michigan population. Can J Fish Aquat Sci 40 (6), 681–698.

Takasuka, A., Nishikawa, H., Furuichi, S., Yukami, R., Revisiting sardine recruitment hypotheses: Egg-production-based survival index improves understanding of recruitment mechanisms of fish under climate variability. Fish and Fisheries, 13, doi: 10.1111/faf.12564.

Tenningen, Maria, Slotte, Aril, Skagen, Dankert, 2011. Abundance estimation of Northeast Atlantic mackerel based on tag recapture data—a useful tool for stock assessment? Fish. Res. 107 (1-3), 68–74.

Trenkel, V.M., Huse, G., MacKenzie, B., Alvarez, P., Arizzabalaga, H., Castonguay, M., Goñi, N., Grégoire, F., Hátún, H., Jansen, T., Jacobsen, J.A., Lehodey, P., Lutcavage, M., Mariani, P., Melvin, G., Nielson, J.D., Nøttestad, L., Óskarsson, G.J., Payne, M., Richardson, D., Senina, I., Speirs, D.G., 2014. Comparative ecology of widely-distributed pelagic fish species in the North Atlantic: implications for modelling climate and fisheries impacts. Prog. Oceanogr. 129, 219–243. https://doi.org/10.1016/j.pocean.2014.04.030.

Tyler, C. R., Sumpter, J. P., 1996. Oocyte growth and development in teleosts. Reviews in Fish Biology and Fisheries 6, 287-318, doi: 10.1007/bf00122584.

Varpe, Øystein, Fiksen, Øyvind, Slotte, Aril, 2005. Meta-ecosystems and biological energy transport from ocean to coast: The ecological importance of herring migration. Oecologia 146 (3), 443–451. https://doi.org/10.1007/s00442-005-0219-9.

Venables, W.N., Ripley, B.D., 2002. Modern Applied Statistics with S, 4th ed. Springer, New York.

Wallace, P.D., 1991. Seasonal variation in fat content of mackerel (Scomber scombrus L.) caught in the western English Channel, Fish. Res. Tech. Rep., MAFF Direct. Fish Res., Lowestoft (91): 8 pp. Fish. Res. Tech. Rep., MAFF Direct. Fish Res., Lowestoft (91): 8 pp, MAFF, Fish. Lab., Pakefield Rd., Lowestoft NR33 0HT, UK.

Walsh, M., Reid, D.G., Turrell, W.R., 1995. Understanding mackerel migration off Scotland - tracking with echosounders and commercial data, and including environmental correlates and behavior. ICES J Mar Sci 52, 925–939.

Ware, D.M., 1977. Spawning time and egg size of atlantic mackerel, *Scomber scombrus*, in relation to plankton. J. Fish. Res. Board. Can 34, 2308–2315.